Cleaved-facet violet laser diodes with lattice-matched $Al_{0.82}In_{0.18}N/GaN$ multilayers as n-cladding

R. Charash' , H. Kim-Chauveau, J-M. Lamy, M. Akther, P. P. Maaskant, E. Frayssinet, P. de Mierry, A. D. Dräger, J-Y. Duboz, A. Hangleiter, and B. Corbett

Citation: Appl. Phys. Lett. **98**, 201112 (2011); doi: 10.1063/1.3589974
View online: http://dx.doi.org/10.1063/1.3589974
View Table of Contents: http://aip.scitation.org/toc/apl/98/20
Published by the American Institute of Physics

Cleaved-facet violet laser diodes with lattice-matched $Al_{0.82}In_{0.18}N/GaN$ multilayers as *n*-cladding

R. Charash,[1,a)] H. Kim-Chauveau,[2] J-M. Lamy,[1] M. Akther,[1] P. P. Maaskant,[1] E. Frayssinet,[2] P. de Mierry,[2] A. D. Dräger,[3] J-Y. Duboz,[2] A. Hangleiter,[3] and B. Corbett[1]
[1]*Tyndall National Institute, University College Cork, Lee Maltings, Cork, Ireland*
[2]*CRHEA-CNRS, Rue Bernard Grégory, Sophia Antipolis, 06560 Valbonne, Prouvènço, France*
[3]*Institute of Applied Physics, Technische Universität Braunschweig, Mendelssohnstrasse 2, D-38106 Braunschweig, Germany*

(Received 14 March 2011; accepted 18 April 2011; published online 19 May 2011)

Electrically injected, edge-emitting cleaved-facet violet laser diodes were realized using a 480 nm thick lattice matched Si doped $Al_{0.82}In_{0.18}N/GaN$ multilayer as the cladding on the *n*-side of the waveguide. Far-field measurements verify strong mode confinement to the waveguide. An extra voltage is measured and investigated using separate mesa structures with a single AlInN insertion. This showed that the electron current has a small thermally activated shunt resistance with a barrier of 0.135 eV and a current which scales according to V^n, where $n \sim 3$ at current densities appropriate to laser operation. © *2011 American Institute of Physics*. [doi:10.1063/1.3589974]

The $Al_{1-x}In_xN$ alloy is of great interest for electronic[1,2] and optoelectronic devices[3–5] due to its large spontaneous polarization fields and its high refractive index contrast with GaN.[7] Conventional visible laser diodes use strained $Al_yGa_{1-y}N$ (with y in the range of 8%) materials as the waveguide cladding layers where thicknesses of >1 μm are required to minimize the leakage of the guided optical modes into the high index GaN substrate. This requirement on layer thickness could be reduced by using $Al_yGa_{1-y}N$ with higher Al composition, but this is not possible due to the excess tensile strain introduced which causes cracking. On the other hand the $Al_{1-x}In_xN$ alloy is lattice matched to GaN for a composition of x=18.4% (Ref. 6) for fully relaxed bulk GaN, thus generating no strain in the heterostructure. Furthermore the 8% refractive index contrast with GaN at 400 nm remains high even at wavelengths of 520 nm where it is 6.25%.[7] For $Al_{0.08}Ga_{0.92}N$ the index contrast with GaN at 400 nm and 520 nm is 1.7% and 0.8%, respectively. Thus, for lasers around 400 nm, a thin AlInN cladding thickness can be used while for longer wavelengths an increased optical mode confinement can be obtained which can compensate the reduced optical gain of InGaN quantum wells (QWs) at those wavelengths.

Incorporation of AlInN into laser structures has not been widely reported due to the difficulty in growing high quality AlInN layers which is associated with the conflicting temperature requirements for the AlN and InN parts of the alloy. Recently reports have been made on optically pumped lasing[8] and on electrically pumped lasing[9,10] where a thin layer of AlInN was used in combination with AlGaN to obtain improved far-field performance. In this letter, we report electrically pumped lasing based on a multilayered AlInN/GaN lower cladding. The current transport properties of the *n*-doped, lattice matched AlInN/GaN multilayered structures are also analyzed.

The structures were grown on a Thomas Swan $3\times2''$ close-coupled showerhead metal-organic chemical-vapor deposition reactor using *c*-plane, *n*-doped free standing GaN substrates with a dislocation density of $\sim 1-2\times10^7$ cm^{-3}. It was found that when growing thick (500 nm) AlInN layers lattice matched with GaN, V-shape pits appear and the surface quality degraded. To combat this, we introduced thin (<10 nm) GaN layers periodically which allowed a smooth growing surface to be maintained. The best results were obtained with AlInN layers with thickness of ~ 50 nm.

The laser structure consists of an eight period, *n*-doped ($Si \sim 7\times10^{18}$ cm^{-3}) multilayer sequence of 54 nm lattice matched $Al_{0.82}In_{0.18}N$ and 6 nm of GaN, a 100 nm *n*-type GaN waveguiding layer, a four period InGaN/GaN quantum well active region, a 10 nm $Al_{0.2}Ga_{0.8}N$: Mg electron blocking layer and a 100 nm *p*-type GaN upper waveguide. The structure was completed by growing a 105 period of $Al_{0.14}Ga_{0.86}N/GaN$: Mg (2.5 nm/2.5 nm) *p*-cladding superlattice followed by a 25 nm Mg-doped *p*-GaN cap layer for electrical contact, where the final 5 nm was p^{++} doped. The calculated optical confinement factor for the structure is 2.25%.

The lasers were realized by forming lines of Pd (50 nm) with different widths ($2-10$ μm) by electron beam evaporation and lift off. Pd acts both as the *p*-contact metallization and as a self-aligned etch mask to define ridge waveguiding structures by Cl_2 based inductively coupled plasma etching (ICP). After defining the ridge, a thin SiO_2 isolation layer was deposited, the oxide was opened on the top of the ridge and a Ti/Au bond-pad metal was evaporated. The samples were then thinned to 100 μm and a Ti/Al/Ti/Au (20/170/5/50 nm) *n*-contact metallization was evaporated on the thinned substrate. No alloying steps were used in the process.

The laser devices were then cleaved to different cavity lengths and the uncoated devices were measured under pulsed conditions (100 ns with 0.1% duty cycle) to avoid device heating. The electroluminescence spectra were collected using a fiber coupled spectrometer and the optical output power using a silicon photodiode from the same facet. Figure 1 shows the light-current density-voltage (L-J-V) characteristics with the inset showing the lasing spectral evolution from a (2×900) μm^2 laser at room temperature. Stimulated emission was observed at the wavelength of

a)Electronic mail: ragh.charash@tyndall.ie.

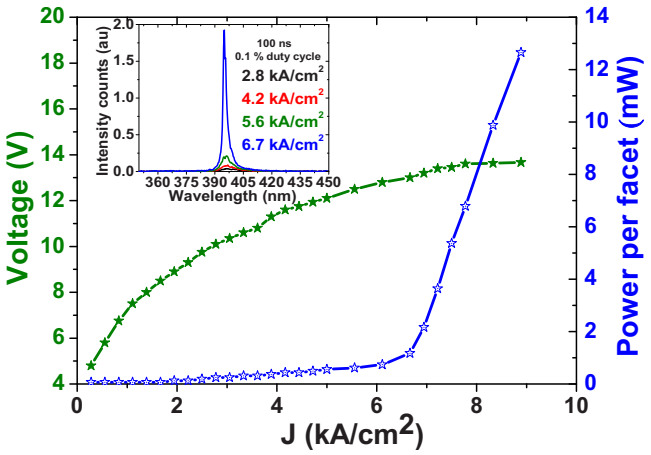

FIG. 1. (Color online) Light-current density-voltage characteristics of a 900 μm long uncoated laser. The inset shows the spectral evolution with current density.

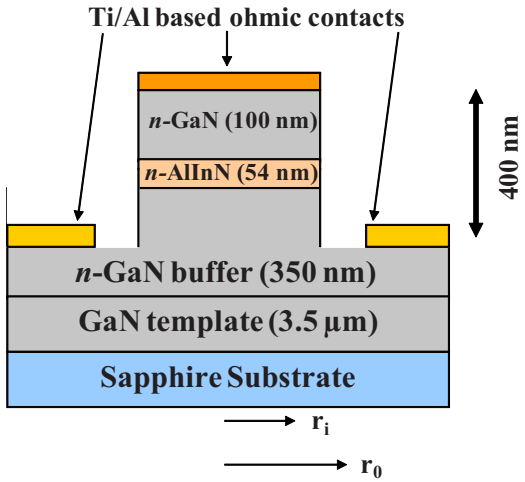

FIG. 3. (Color online) Schematic of the GaN/AlInN/GaN structure used to study the vertical current transport (r_i=12.5 μm, r_o=32.5 μm).

~394 nm with a threshold current density of 6.7 kA/cm^2.

Figure 2 shows the comparison and the reasonable agreement between the measured vertical far-field laser emissions from an output facet with the simulated far-field which used a refractive index of 2.334 for the AlInN. It is evident from the far-field measurement that there is no mode leakage into the substrate and that the *n*-AlInN/GaN multistack acts as an excellent optical blocking layer due to its large refractive index contrast with the active region. The far-field from a reference laser which had a 150 period of $Al_{0.15}Ga_{0.85}N$/GaN, 2.56 nm/2.6 nm cladding on the *n*-side is compared with the laser with the AlInN/GaN cladding in the inset. Mode leakage in the AlGaN clad laser is evident as a perturbation in the far-field. This feature is problematic for such lasers to be used in display applications. The wider vertical divergence of laser diodes with AlInN *n*-waveguide cladding layers compared to laser diodes with AlGaN *n*-waveguide cladding layers confirms that AlInN offers tight mode confinement.

The electrical measurements show an excess voltage for the laser diodes with AlInN cladding. An excess voltage may be expected as the heterointerface between AlInN and GaN has a large conduction band offset which is suggested to be as large as 1 eV (Ref. 11) which will lead to a strong barrier

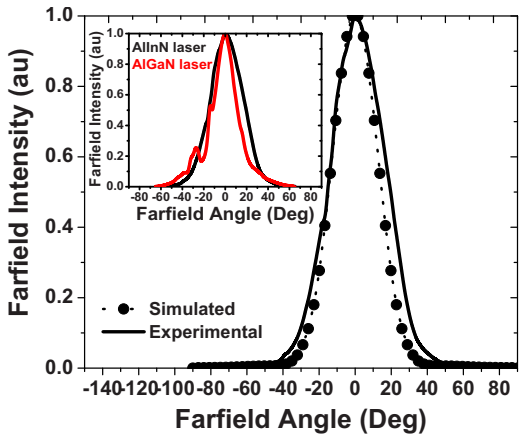

FIG. 2. (Color online) Measured and calculated vertical far-field from the laser. The substrate is to the left of the waveguide region. The inset shows a comparison of the far-fields from lasers with AlInN and AlGaN *n*-waveguide cladding layers.

for the transport of electrons. In order to understand this and the nature of the current transport through such structures, an *n*-type (Si) test structure containing a single AlInN layer was investigated. The single Si-doped ($\sim 7\times10^{18}$ cm^{-3}) 54 nm thick AlInN layer was grown on an *n*-GaN buffer layer (350 nm) on a 3.5 μm thick GaN template on sapphire and was completed with a 100 nm of *n*-GaN. Circular mesas of different diameters were etched to the buffer layer with Ti/Al/Ti/Pd (20/170/5/50 nm) as the upper *n*-type metal contact (Fig. 3). The Pd was used as the etch mask using ICP. Ti/Al/Ti/Au (20/170/5/50 nm) was deposited on the etched surface as a lower Ohmic contact with a gap of 20 μm between the mesa and the bottom contact. The contacts were alloyed at 750 °C. Four point circular transmission line measurements on both the contacts revealed Ohmic contacts with specific contact resistance values better than 3×10^{-5} Ω cm^2 and 1×10^{-6} Ω cm^2, respectively. The measured sheet resistance of the upper and lower layers is 186 Ω/sq and 21 Ω/sq, respectively.

The current-voltage characteristics were measured for vertical transport across the GaN–AlInN–GaN interfaces for different diameter mesas (10–200 μm) as a function of temperature (0–200 °C). The current is found to scale with the area of the mesa at low bias ($V<0.1$ V) but not at higher biases ($V>0.1$ V). At the higher biases the current is found to scale according to the perimeter length of the mesa multiplied by a current spreading length, L, where L is found to be in the range of 10–20 μm. This can be explained as the current being through a shunt resistance at low bias (see below) and across a diode-like structure at higher bias. The origin of this diode-like behavior is the heterointerfaces between AlInN and GaN. In that case, due to current crowding, a current spreading length can be estimated from[12] $L_s=\sqrt{(\rho_c+R_{top}^{sheet}t_{top}^2)/R_{bottom}^{sheet}}$, where ρ_c-the specific contact resistivity of the top contact, t_{top}-the thickness of the top GaN layer, R_{top}^{sheet} and R_{bottom}^{sheet} represent the sheet resistances of the top layer and the remaining buffer layer left after etching. From the measured data L is calculated to be 12 μm.

This shows that the current injection in the laser is homogeneous (ridge width of 2–10 μm) and reasonably homogeneous in the test structure used below (25 μm diameter). Figure 4 shows the forward bias (applied to the top of

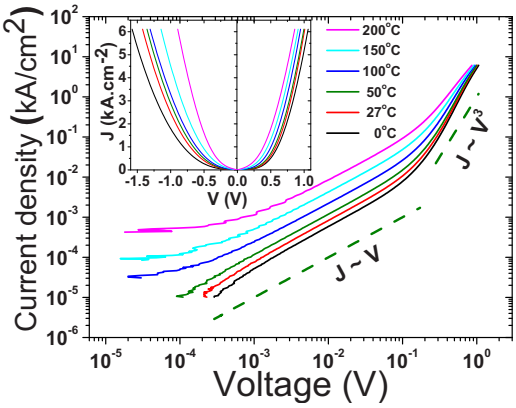

FIG. 4. (Color online) Temperature dependent forward bias-current density curves from a 25 μm diameter GaN/AlInN/GaN cylindrical mesa. A linear and cubed dependence of the current density on voltage is shown for reference. The inset shows the temperature dependent forward and reverse bias curves for the same device on a linear scale.

the mesa) temperature dependent current density against voltage for a 25 μm diameter mesa. The data is plotted in a log-log scale in order to reveal the two different regimes and the power dependence between J and V. At low bias ($V < 0.1$ V) the current transport is resistive ($J = V/R$) with a strong temperature dependence for the resistance, R. This is a shunt across the interfaces probably associated with defects. The resistivity can be parametrized as $R = Ro \exp(\phi/kT)$ with the barrier height, ϕ being 0.135 eV. We interpret this as the resistivity of the AlInN layer reducing with temperature due to ionization of donors which is in line with a recent report of a trap state in AlInN being 0.12 eV below the conduction band edge.[13] At higher voltages the current density scales as V^n with $n \sim 3$. The temperature dependence is much less suggesting a tunnel component to this current. There is a voltage penalty of about 0.8 V at carrier densities appropriate to lasing (6 kA/cm^2). Note that in actual laser structures the number of AlInN/GaN stacks is 8, leading to an expected excess voltage of 6.4 V, in qualitative agreement with the result in Fig. 1. We have observed a reduction in the excess voltage with poor quality (V-pits) AlInN cladding layers, suggesting the possible role of V-pits as short circuits. This, however, is at the expense of degraded QWs and larger optical losses, and therefore cannot be used as a solution for reducing the excess voltage.

The inset in Fig. 4 shows the same forward data along with the reverse J-V data presented on a linear scale. This shows a small asymmetry between the forward and reverse directions of current flow and the asymmetry reduces with temperature. Since the current is due to electron transport across each GaN–AlInN in turn, this suggests that there is a small built-in asymmetry between the band structure at the upper and lower interfaces which is overcome at higher temperatures where thermionic emission transport dominates.

In summary, we have achieved lasing with an *n*-type AlInN/GaN multistack lower waveguide cladding. Vertical far-field measurements showed that AlInN is very effective in confining the mode; it is superior to the use of thick AlGaN. Current transport through the AlInN is due to a temperature activated shunt resistance and a tunnel-like current at lasing current densities. The need to use multiple AlInN layers to maintain good crystalline quality results in an additional voltage drop in the device. The voltage drop can be decreased by increasing the doping level, grading the interfaces or by making intracavity contacts to the *n*-guide region.

This work has been supported by Enterprise Ireland (Contract No. IRF/08/SPOT/14), the French project ANR-MATETPRO Truegreen and by the European Regional Development Fund through the ERA-SPOT program.

[1]J. Kuzmík, IEEE Electron Device Lett. **22**, 510 (2001).
[2]J. Kuzmík, Semicond. Sci. Technol. **17**, 540 (2002).
[3]H. P. D. Schenk, R. Czernecki, K. Krowicki, G. Targowski, S. Grzanka, M. Krysko, P. Prystawko, P. Wisniewski, M. Leszczynski, H. Teisseyre, G. Franssen, J. Muszalski, T. Suski, and P. Perlin, Phys. Status Solidi C **1**, 1537 (2004).
[4]E. Feltin, J.-F. Carlin, J. Dorsaz, G. Christmann, R. Butté, M. Laügt, M. Ilegems, and N. Grandjean, Appl. Phys. Lett. **88**, 051108 (2006).
[5]R. Butté, J.-F. Carlin, E. Feltin, M. Gonschorek, S. Nicolay, G. Christmann, D. Simeonov, A. Castiglia, J. Dorsaz, H.-J. Buehlmann, S. Christopoulos, G. Baldassarri Höger von Högersthal, A. J. D. Grundy, M. Mosca, C. Pinquier, M. A. Py, F. Demangeot, J. Frandon, P. G. Lagoudakis, J. J. Baumberg, and N. Grandjean, J. Phys. D **40**, 6328 (2007).
[6]V. Darakchieva, M. Beckers, M.-Y. Xie, L. Hultman, B. Monemar, J.-F. Carlin, E. Feltin, M. Gonschorek, and N. Grandjean, J. Appl. Phys. **103**, 103513 (2008).
[7]T. Lermer, M. Schillgalies, A. Breidenassel, D. Queren, C. Eichler, A. Avramescu, J. Müller, W. Scheibenzuber, U. Schwarz, S. Lutgen, and U. Strauss, Phys. Status Solidi A **207**, 1328 (2010).
[8]H. P. D. Schenk, M. Nemoz, M. Korytov, P. Vennéguès, P. Demolon, A. D. Dräger, A. Hangleiter, R. Charash, P. P. Maaskant, B. Corbett, and J. Y. Duboz, Phys. Status Solidi C **6**, S897 (2009).
[9]A. Castiglia, E. Feltin, G. Cosendey, A. Altoukhov, J.-F. Carlin, R. Butté, and N. Grandjean, Appl. Phys. Lett. **94**, 193506 (2009).
[10]A. Castiglia, J.-F. Carlin, E. Feltin, G. Cosendey, J. Dorsaz, and N. Grandjean, Appl. Phys. Lett. **97**, 111104 (2010).
[11]M. Akazawa, T. Matsuyama, T. Hashizume, M. Hiroki, S. Yamahata, and N. Shigekawa, Appl. Phys. Lett. **96**, 132104 (2010).
[12]X. Guo and E. F. Schubert, J. Appl. Phys. **90**, 4191 (2001).
[13]E. Arslan, S. Bütün, and E. Ozbay, Appl. Phys. Lett. **94**, 142106 (2009).